

# Implementing homo- and heterodecoupling in region-selective HSQMBC experiments



Laura Castañar, Josep Saurí, Pau Nolis, Albert Virgili, Teodor Parella \*

Servei de Ressonància Magnètica Nuclear and Departament de Química, Universitat Autònoma de Barcelona, E-08193 Bellaterra (Catalonia), Spain

## ARTICLE INFO

### Article history:

Received 21 September 2013

Revised 27 October 2013

Available online 15 November 2013

### Keywords:

Pure-shift

Band-selective HSQMBC

Proton–carbon coupling constants

Homonuclear decoupling

Sensitivity improvement

Resolution enhancement

## ABSTRACT

An NMR method to enhance the sensitivity and resolution in band-selective long-range heteronuclear correlation spectra is proposed. The excellent in-phase nature of the selHSQMBC experiment allows that homonuclear and/or heteronuclear decoupling can be achieved in the detected dimension of a 2D multiple-bond correlation map, obtaining simplified cross-peaks without their characteristic fine J multiplet structure. The experimental result is a resolution improvement while the highest sensitivity is also achieved. Specifically, it is shown that the  $^1\text{H}$ -homodecoupled band-selective (HOBS) HSQMBC experiment represents a new way to measure heteronuclear coupling constants from the simplified in-phase doublets generated along the detected dimension.

© 2013 Elsevier Inc. All rights reserved.

## 1. Introduction

Long-range heteronuclear correlation experiments are key NMR tools for the structural characterization of small molecules and natural products in solution. The widely used HMBC/HSQMBC pulse schemes have been modified in several ways in order to improve their success application on a wide range of issues [1–2]. For instance, band-selective excitation in the indirect carbon dimension allows use very reduced spectral widths, and therefore the resolution/dispersion between  $^{13}\text{C}$  signals can be strongly increased [3–7]. On the other hand, different attempts have been made to remove the undesired effects due to the evolution of  $J(\text{HH})$  that generate cross-peaks with complex phase multiplets. This is particularly severe in HMBC experiments because  $J(\text{HH})$  evolves during all the evolution periods, yielding an additional characteristic skew of the cross-peaks that can compromise peak analysis. Constant-time versions of the HMBC experiment have been proposed to remove such inconvenience and their combination with band-selective excitation affords better defined spectra [8–9]. It has been shown that pure-phase cross-peaks can be obtained from HSQMBC experiments using region-selective  $180^\circ$   $^1\text{H}$  pulses at the middle of the INEPT periods [10–11]. The excellent in-phase (IP) multiplet structure with respect to  $J(\text{HH})$  allows the quantitative and accurate measurement of  $^jJ(\text{CH})$  from non-distorted pure-phase multiplets along the detected dimension. Furthermore, the easy implementation of the IPAP methodology

affords a powerful way to extract them, even when J coupling values are smaller than the linewidth, by analyzing the relative displacement between separate  $\alpha/\beta$  multiplet components [10].

On the other hand, the concept of pure-shift NMR has been introduced in multidimensional NMR experiments as a method to simplify the  $J(\text{HH})$  multiplet structure of proton resonances [12–21]. Most of these experiments rely in spatial encoding selection and their reliable applicability strongly depends on the experimental sensitivity. For this reason, pure-shift experiments have been mainly reported for homonuclear applications because its implementation into heteronuclear inverse-detected experiments suffers of important sensitivity success. Using a different concept, a tilted pseudo-3D HMBC experiment has been proposed to achieve  $^1\text{H}$ -homodecoupling along the detected dimension by incorporating a J-resolved dimension into the HMBC pulse scheme [22].

Recently, a new detection scheme to obtain HOmodecoupled Band-Selection (HOBS) in the detected dimension of multidimensional NMR experiments has been reported [23]. It has been successfully implemented in homonuclear (TOCSY) and heteronuclear (HSQC) experiments involving in-phase HH magnetization. However, the incorporation of this technique in experiments involving anti-phase HH magnetization, like the regular COSY, HMBC or HSQMBC experiments, fail because the evolution of  $J(\text{HH})$  generates anti-phase components that would cancel under homodecoupling conditions. Here we show how the HOBS methodology can be implemented in the pure-phase selHSQMBC experiment in order to obtain pure-shift heteronuclear correlation spectra that offer a considerable enhancement in both resolution

\* Corresponding author.

E-mail address: [teodor.parella@uab.cat](mailto:teodor.parella@uab.cat) (T. Parella).

and sensitivity. In addition, the method is also fully compatible with band-selective excitation in the indirect dimension and with broadband heteronuclear decoupling during detection to obtain high-resolved pure-shift region-selective HSQMB spectra. It will be shown that the method is also amenable to measure small heteronuclear coupling constants from the pure-phase doublet cross-peaks originated along the detected dimension and also fully compatible with the IPAP methodology described early [24]. All these features will be illustrated using the cyclic undecapeptide cyclosporine as test sample.

## 2. Results and discussion

Fig. 1 displays two basic pulse schemes of the selHSQMB experiment [10] that incorporates band-selective homodecoupling during the acquisition period using the HOBS technique. Fig. 1A is a conventional experiment offering broadband  $^{13}\text{C}$  excitation in the indirect dimension, whereas Fig. 1B is a  $^{13}\text{C}$  band-selective version where the original  $G1-180^\circ(^{13}\text{C})-\delta$  period during the  $t_1$  period has been replaced by a  $G1*0.5-180^\circ(^{13}\text{C}_{\text{sel}})-G1*(-0.5)$  block. As in the original experiment, the region-selective  $180^\circ$   $^1\text{H}$  pulses applied on non-mutually coupled protons during the long INEPT delays avoid any  $J(\text{HH})$  evolution. Just prior to acquisition, signals present pure IP properties with respect to  $J(\text{HH})$  coupling constants that are amenable for the application of the HOBS detection

scheme to collapse the multiplet  $J$  structure. The HOBS scheme consists of  $n$  concatenated loops that includes a pair of hard/region-selective  $180^\circ$   $^1\text{H}$  pulses (each one flanked by the  $G3$  and  $G4$  gradients) applied at intervals of  $2\Delta$  period ( $\Delta$  is set to  $AQ/2n$ ) as shown in the box of Fig. 1. The selective  $180^\circ$  pulses applied in the INEPT and during detection have the same shape and duration, minimizing the requirements for additional experimental set-up. Thus, all protons selected by the region-selective  $180^\circ$   $^1\text{H}$  pulse appear homodecoupled from all other protons that do not experience this pulse, and the result is a band-selective homodecoupled observation of a specific region of the  $^1\text{H}$  spectrum. The method is also fully compatible with optional broadband heteronuclear  $^{13}\text{C}$  decoupling which is applied only during the FID acquisition periods ( $\Delta$ ), as shown in Fig. 1. We refer to this technique as a BEHOBS (Broadband-hEterodecoupled and HOmodecoupled Band-Selective) and it affords fully homo- and heteronuclear decoupled spectra consisting only of singlet cross-peaks.

Fig. 2A shows the refocused IP version of the conventionally detected selHSQMB spectrum of cyclosporine after applying a 5 ms REBURP  $180^\circ$  pulse as a band-selective  $180^\circ$   $^1\text{H}$  pulse on its  $\text{H}_\alpha$  proton region [10–11]. Clearly, all expected long-range correlations are observed showing perfect IP multiplets with respect to both  $J(\text{HH})$  and  $J(\text{CH})$  coupling constants along the detected dimension. Fig. 2B shows the analog HOBS-HSQMB spectrum acquired using the scheme of Fig. 1A but without heteronuclear decoupling. We

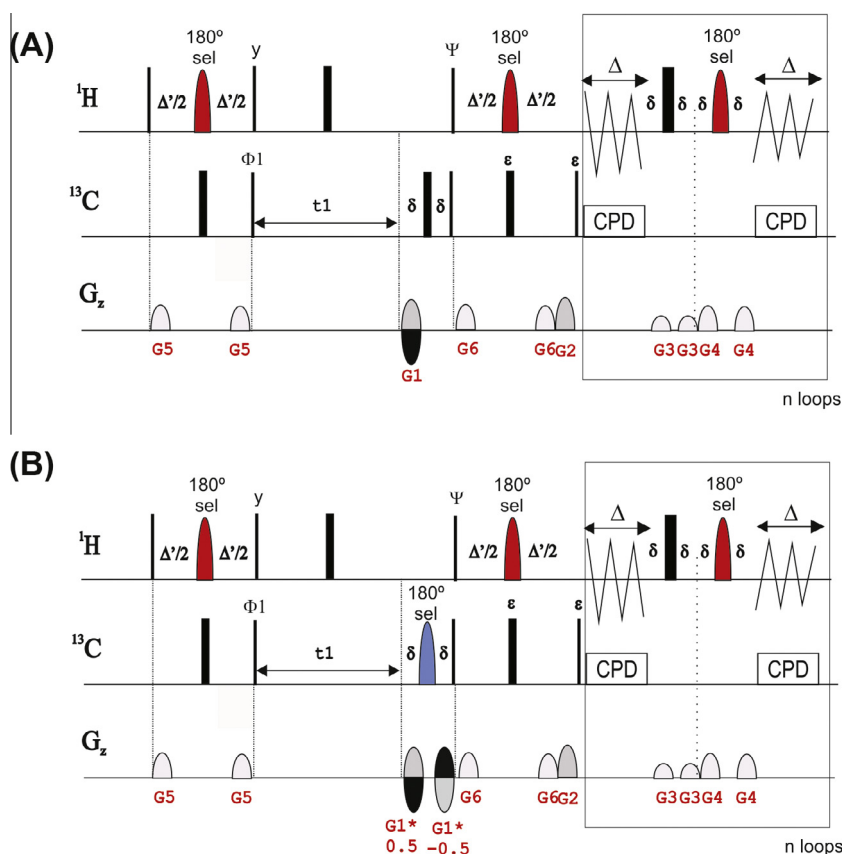


**Fig. 1.** Experimental pulse schemes for the (A)  $^{13}\text{C}$ -broadband and (B)  $^{13}\text{C}$  region-selective HOBS-HSQMB experiment. Thin and thick bars represent broadband  $90^\circ$  and  $180^\circ$  pulses, respectively, whereas shaped pulses are region-selective  $180^\circ$  pulses. The selective  $180^\circ$   $^1\text{H}$  pulse applied at the middle of INEPT periods and during detection have the same shape and duration ( $p_{180}$ ) and we found that REBURP pulses in the order of 3–10 ms provides the best result as a function of the required selectivity. The INEPT delays are set to  $\kappa = \Delta' + p_{180} = 1/(2 * J_{\text{CH}})$ . The basic phase cycling is  $\Phi_1 = x, -x$  and  $\Phi(\text{receiver}) = x, -x$ ; all other unlabeled pulses are from the  $x$ -axis. Homonuclear decoupling during the acquisition time ( $AQ$ ) is performed using a refocusing blocks including a pair of hard/selective  $180^\circ$   $^1\text{H}$  pulses applied at intervals of  $2\Delta = AQ/n$ , where  $n$  is the number of loops. Optional heteronuclear decoupling (CPD) during data collection can also be applied as shown in the scheme. For the measurement of proton-carbon coupling constants, the IPAP methodology can be applied: two different IP and AP data are recorded without heteronuclear decoupling as a function of the last  $90^\circ$  and  $180^\circ$   $^{13}\text{C}$  pulses (IP:  $\Psi = y, \varepsilon = \text{on}$ ; AP:  $\Psi = x, \varepsilon = \text{off}$ ) and then they are added/subtracted to afford to separate  $\alpha/\beta$  subspectra. More details in the experimental section.

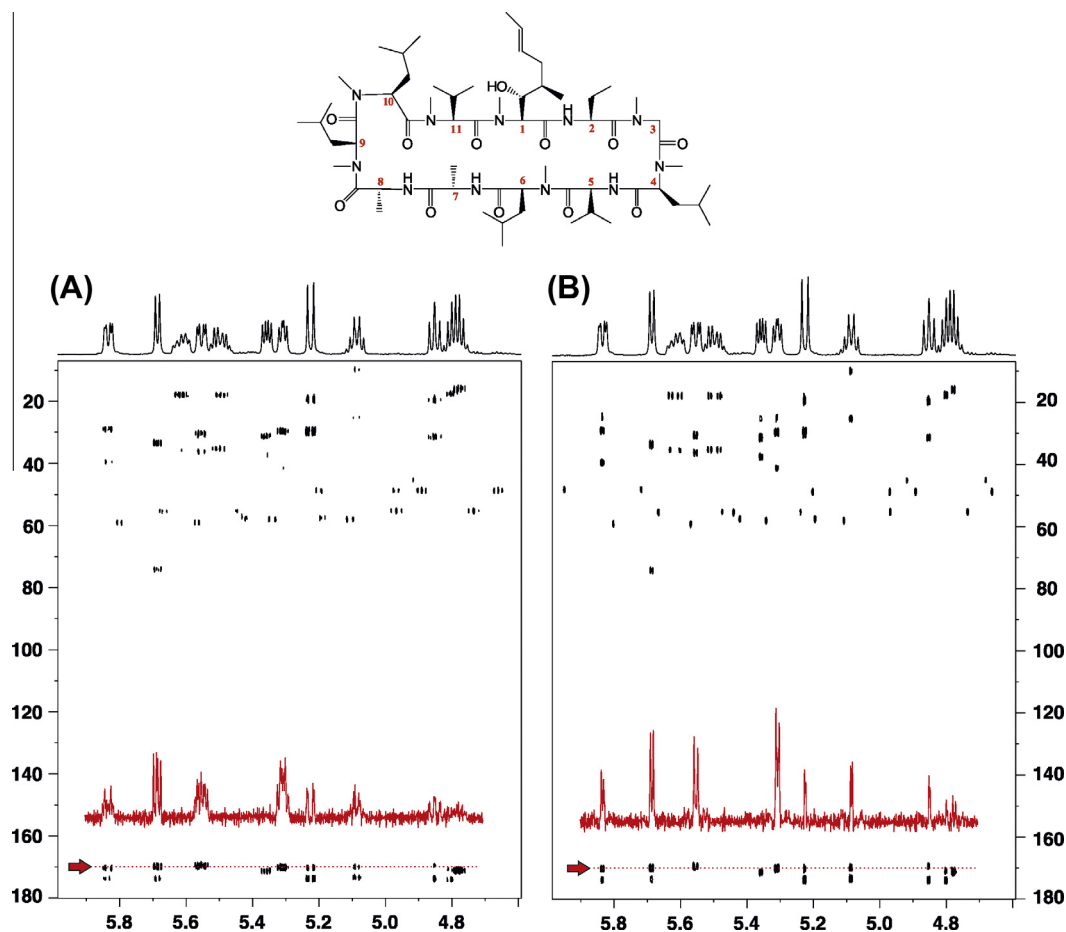


**Fig. 2.** Practical effects of broadband homodecoupling in the selHSQMBC experiment: (A) Conventional and (B) HOBS HSQMBC spectra of cyclosporine acquired under the same experimental time of 20 min. A selected 1D slice is plotted for each spectrum at the same absolute scale to compare the relative sensitivity and resolution achieved in the 2D spectra. The standard 1D spectrum is shown on top of the 2D plot.

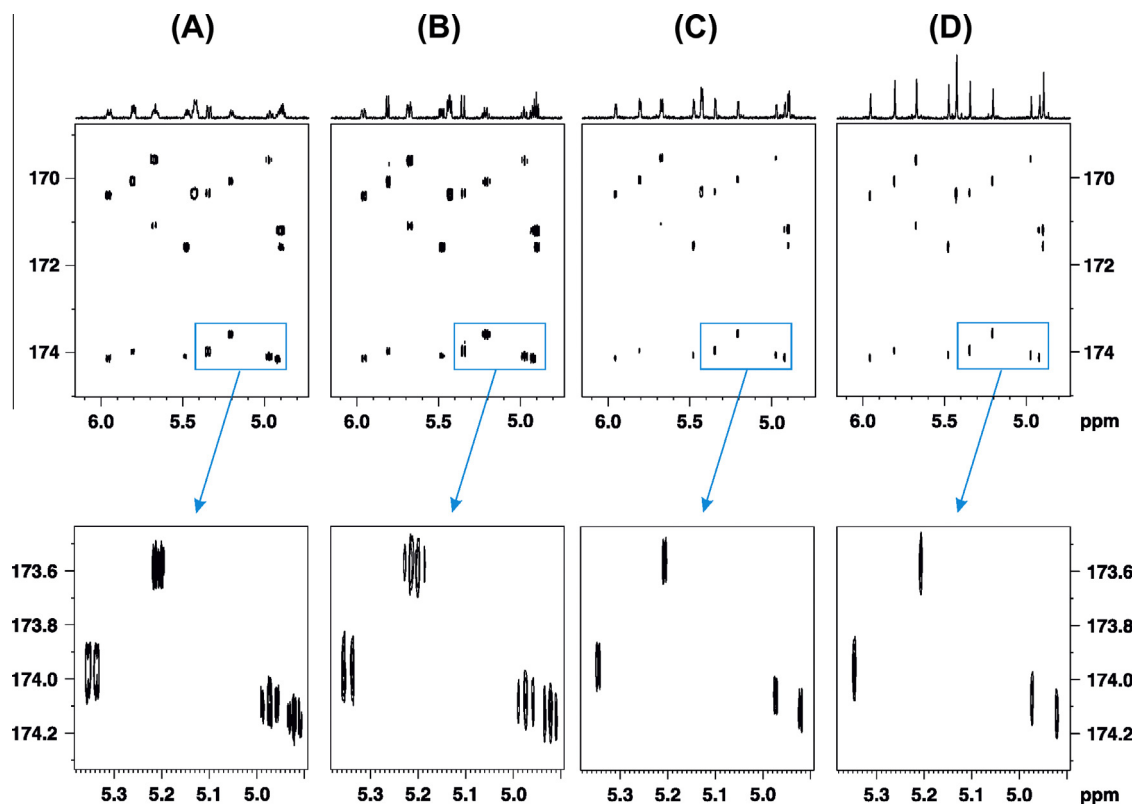
can observe how the  $J(\text{HH})$  multiplet structures of all  $\text{H}_\alpha$  resonances along the detected dimension are collapsed because of the effective homodecoupling of  $\text{H}_\alpha\text{-NH}$  and  $\text{H}_\alpha\text{-H}_\beta$  coupling constants. A more detailed analysis of a 1D row reveals the enhanced resolution and improved sensitivity achieved with the simple implementation of the HOBS technique.

Fig. 3 shows the improved spectral resolution achieved after combining the band-selective  $^{13}\text{C}$  excitation of the carbonyl region in conjunction with the HOBS detection scheme, with simultaneous application of homo- and/or heteronuclear decoupling during data acquisition (see pulse scheme of Fig. 1B): non-decoupled (Fig. 3A), with  $^{13}\text{C}$ -decoupling (BEBS, Fig. 3B), with  $^1\text{H}$ -decoupling (HOBS, Fig. 3C) and with simultaneous  $^{13}\text{C}$  and  $^1\text{H}$ -decoupling (BE-HOBS, Fig. 3D) HSQMBC spectra. The analysis of 1D row confirms the enhanced resolution and the improved sensitivity by gradual  $J$  multiplet simplification, without affecting spectral quality (Fig. 4). The individual analysis of the SNR for each of the observed 19 cross-peaks affords an average enhancement by factors of 1.2 (with heteronuclear decoupling), 1.6 (with homonuclear decoupling) and 2.4 (with both homo- and heteronuclear decoupling) when compared with fully coupled data (normalized average factor of 1).

Of particular interest is the HOBS-HSQMBC spectrum (Fig. 3C) because all cross-peaks are present as pure IP doublets along the F2 dimension. This represents a completely new way to measure coupling constants, because all cross-peaks appear homodecou-

pled from other protons resonating outside of the selected area, and therefore they only display the active  $^1J_{\text{CH}}$  splitting (Fig. 5). The direct extraction of these couplings can be made by direct analysis of cross-peaks if the multiplet is resolved enough. Because we are dealing with band-selective experiments, the spectral width in the direct dimension can be set to a reduced value and therefore, it is relatively easy to achieve high levels of spectral resolution. It can be shown that direct CH correlations are also observed because any low-pass  $J$  filtering method is applied, and therefore the magnitude of one-bond proton–carbon coupling constants,  $^1J(\text{CH})$ , can be determined from the well separated singlet satellite lines. Until now, these scalar  $^1J(\text{CH})$  and residual dipolar  $^1D(\text{CH})$  coupling constants have been measured from F1- or F2-coupled HSQC experiments [25–29] but the advent of new pure-shift NMR methods will offer a new way to perform this [30–32].

In cases of poor resolved multiplets or when the accuracy of the measurements may be doubtful, the IPAP methodology can offer a better solution. The technique is based in the acquisition of separate IP and AP data as a function of the application of the last  $90^\circ$  and  $180^\circ$   $^{13}\text{C}$  pulses in schemes of Fig. 1 (labeled with  $\epsilon$ ) followed by time domain IP  $\pm$  AP data addition/subtraction. In this way, each individual  $\alpha$  and  $\beta$  component of the doublet is obtained in two separate subspectra, rendering the measurement easier by simple determination of their relative mutual shift (Fig. 6). Table 1 shows a perfect agreement between the  $J(\text{CH})$  values measured directly from the proposed HOBS and HOBS-IPAP methods with those ex-



**Fig. 3.** Resolution enhancement effects after incorporation of homo or/and heteronuclear decoupling in region-selected  $^1\text{H}_\alpha$ - $^{13}\text{C}$ O HSQMBBC spectra of cyclosporine: (A) conventional; (B) broadband  $^{13}\text{C}$ -decoupled (BEBS); (C)  $^1\text{H}$ -decoupled (HOBS) and (D)  $^1\text{H}$  and broadband  $^{13}\text{C}$ -decoupled (BEHOBS). The internal projection along the detected dimension is shown on top of each 2D plot and all they are plotted with the same absolute scale to compare the relative sensitivity and resolution.

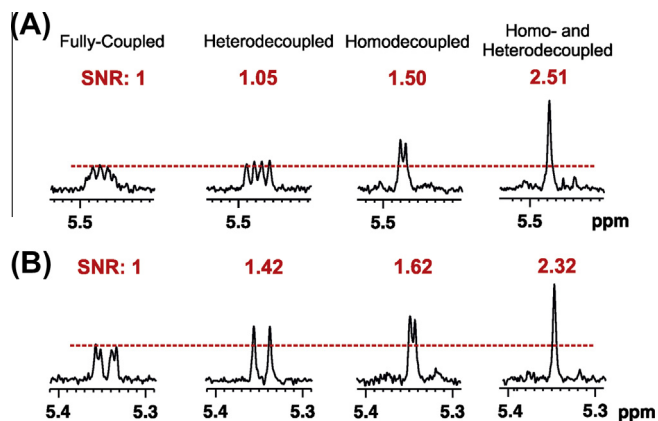


**Fig. 4.** 1D multiplets corresponding to the (A) C6H $\alpha$ 6 and (B) C11H $\alpha$ 11 cross-peaks obtained from the four different HSQMBBC spectra of Fig. 3. The experimental SNR for each signal is shown taking the fully coupled peak (normalized value set to 1) as a reference.

tracted from HSQMBBC-TOCSY spectra [33]. The simplicity of the resulting cross-peaks and their IP nature allows an automated peak picking and an easy extraction of  $^n\text{J}(\text{CH})$  values.

### 3. Conclusions

To conclude, a new method to obtain  $^1\text{H}$ -homodecoupled long-range  $^1\text{H}$ - $^{13}\text{C}$  correlations from a selected area of a 2D spectrum has been developed. The method is fully compatible with simultaneous heteronuclear decoupling, leading to pure-shift NMR spec-

tra, with enhanced resolution and maximum sensitivity. HOBS experiments have the restriction that full broadband homodecoupling can only be accomplished in regions containing non-mutually J coupled protons. As shown for cyclosporine, peptides are excellent targets for their success because NH,  $\text{H}_\alpha$  and other aliphatic protons resonate in characteristic regions of the  $^1\text{H}$  spectrum and there is usually no J interference between them. Alternatives to obtain HOBS spectra for the complete  $^1\text{H}$  spectral range could be feasible by applying spatial-encoded techniques, as reported for broadband Zangger-Sterk (ZS) techniques [14–17], but this would be related to significant reductions in sensitivity.

In addition, we have focused on the success measurement of long-range heteronuclear coupling constants from the resulting in-phase doublet signals along the high-resolved direct dimension. Implementation of the HOBS and related techniques to other experiments is under development and the application to determine coupling constants from ultra simplified multiplets will be further evaluated.

### 4. Experimental

NMR experiments were performed on a Bruker Avance 600 spectrometer (Bruker Biospin, Rheinstetten, Germany) equipped with TXI HCN z-grad probes. The temperature for all measurements was set to 298 K. All spectra were recorded on a 25 mM sample of cyclosporine in  $\text{C}_6\text{D}_6$  and processed with TOPSPIN 2.1 (Bruker Biospin, Rheinstetten, Germany).

The conventional 2D  $^1\text{H}$ - $^{13}\text{C}$  region-selective HSQMBBC spectrum of Fig. 2A was recorded using the pulse scheme of Fig. 1A with a normal detection period [10]. The recycle delay was 1 s,

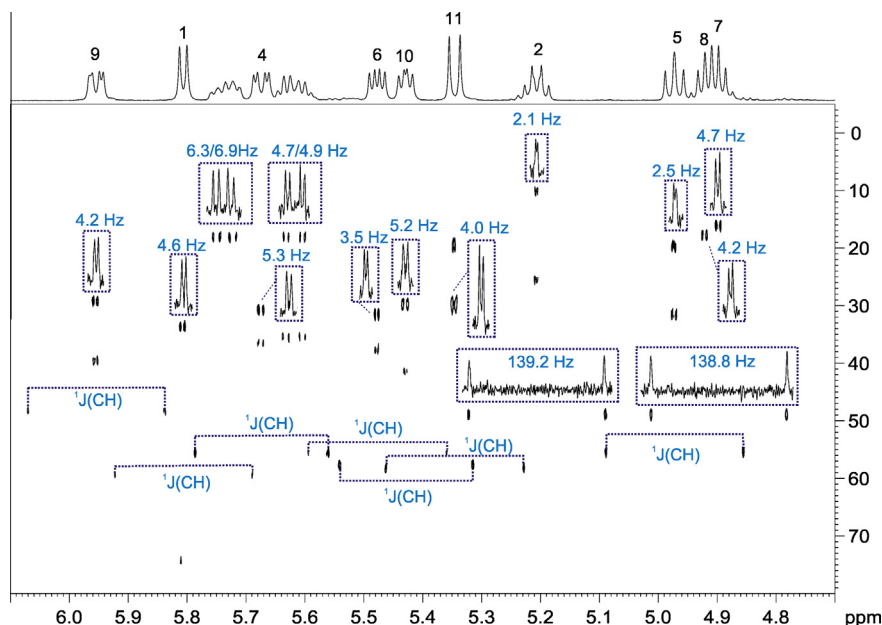


**Fig. 5.** In-phase HOBS-HSQMBC spectra of cyclosporine showing how the value of  $J(\text{CH})$  for all direct and long-range cross-peaks can be extracted directly from the analysis of the clean doublet along the detected dimension (see the extracted value in each individual 1D inset). Note that only the AB spin system (protons resonating at 5.62 and 5.73 ppm) appears as a double of doublets due to their mutual  $J(\text{HH})$ .

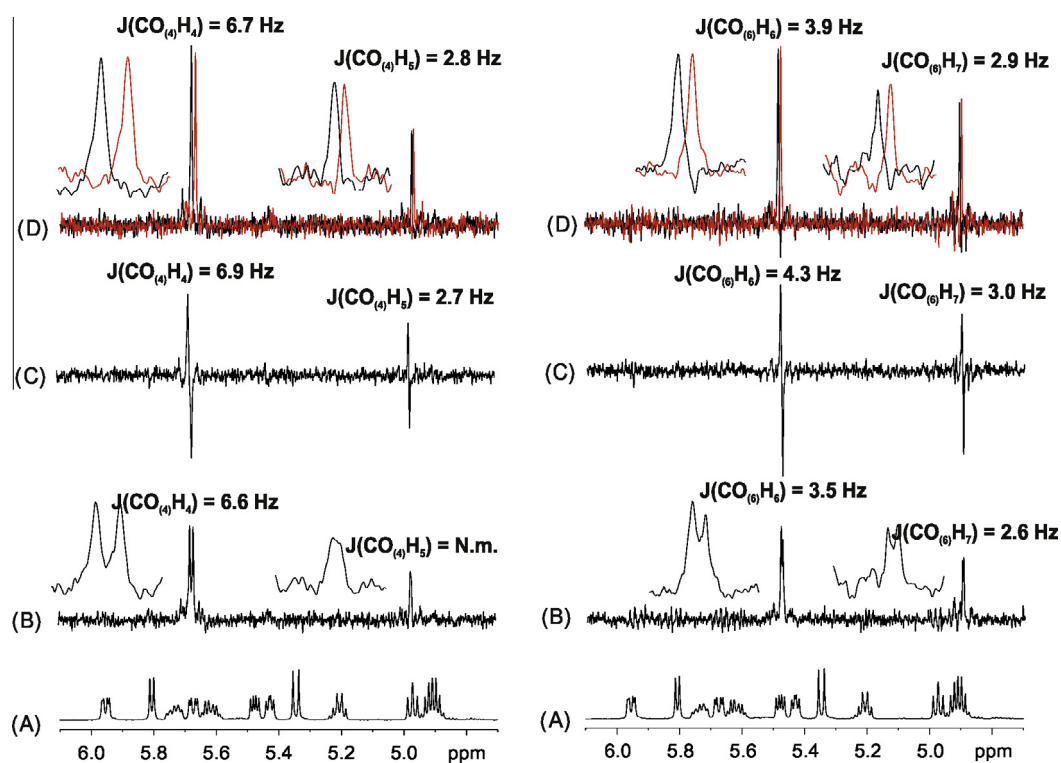


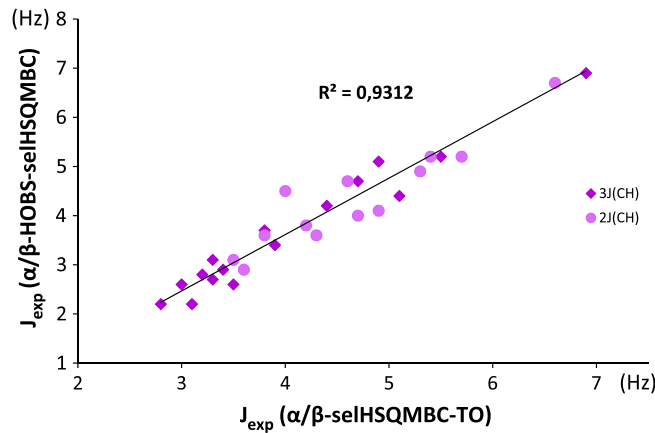
**Fig. 6.**  $\alpha/\beta$  HOBS-HSQMBC spectra of cyclosporine after applied the IPAP technology. The separate  $\alpha$  and  $\beta$  sub-spectra generated after a combination  $\text{IP} \pm \text{AP}$  are overlaid in black/red colors to distinguish the relative shifts along the detected dimension. (B–D) are 1D slices extracted at two different  $\text{CO}(4)$  (169.5 ppm) and  $\text{CO}(6)$  (171.6 ppm) carbonyl frequencies corresponding to the (B) in-phase, (C) anti-phase and (D)  $\alpha/\beta$  multiplets. (For interpretation of the references to color in this figure legend, the reader is referred to the web version of this article.)

the region-selective  $180^\circ$   $^1\text{H}$  pulse was a REBURP shape of 5 ms of duration ( $p_{180}$ ), and the interpulse INEPT delays ( $\kappa = \Delta' + p_{180} = 1/(2 * {}^nJ_{\text{CH}})$ ) were optimized for 8 Hz. 4 scans were accumulated for each one of the 128  $t_1$  increments, the spectral windows in F1 and F2 dimensions were 30,180 Hz and 1800 Hz,

respectively, the number of data points in  $t_2$  was set to 4096 and the acquisition time (AQ) was 1.13 s. The total experimental time was of 20 min. The ratio between the G1:G2:G3:G4:G5:G6 gradients were 80:20.1:41:63:11:17, measured as percentage of the absolute gradient strength of 53.5 G/cm. Data were acquired and



**Table 1**  
Proton-carbon coupling constant values (in Hz) in cyclosporine measured from the (A) in-phase HOBS-selHSQMBC, (B) IPAP HOBS-selHSQMBC, and (C) IPAP selHSQMBC-TOCSY [33] experiments. Only the small two- and three-bond proton-carbon coupling constants marked in grey have been represented in the upper graph. The experimental error was of ±0.4 Hz.



J(C-H <sub>α</sub> )	IP HOBS-selHSQMBC (in Hz)	α/β HOBS-selHSQMBC (in Hz)	α/β selHSQMBC-TOCSY (in Hz)
<sup>3</sup> JC2γ-H2	2.1	2.6	3.0
<sup>2</sup> JC7β-H7	4.7	4.7	4.6
<sup>3</sup> JC1η-H1a(olef)	6.3	6.9	6.9
<sup>2</sup> JC1η-H1b(olef)	4.7	4.9	5.3
<sup>2</sup> JC8β-H8	4.2	4.5	4.0
<sup>3</sup> JC11γ-H11	2.0	2.2	2.8
<sup>3</sup> JC5γ-H5	2.5	3.1	3.3
<sup>3</sup> JNMe-H9	4.2	4.4	5.1
<sup>3</sup> JNMe-H10	5.2	5.2	5.5
<sup>3</sup> JNMe-H11	4.0	4.2	4.4
<sup>3</sup> JNMe-H4	5.3	5.1	4.9
<sup>3</sup> JNMe-H6	3.5	3.7	3.8
<sup>2</sup> JC5β-H5	4.1	4.1	4.9
<sup>3</sup> JNMe-H1	4.6	4.7	4.7
<sup>1</sup> JC8H8	142.5	142.2	–
<sup>1</sup> JC9H9	139.3	139.2	139.5
<sup>1</sup> JC2H2	139.2	139.1	138.9
<sup>1</sup> JC7H7	138.8	138.1	–
<sup>1</sup> JC5H5	139.6	139.6	–
<sup>1</sup> JC4H4	135.8	135.6	135.9
<sup>1</sup> JC11H11	140.4	140.4	140.3
<sup>1</sup> JC10H10	135.5	135.6	135.8
<sup>1</sup> JC6H6	141.1	141.0	–
<sup>1</sup> JC1H1	139.9	139.8	140.1
<sup>2</sup> JCO4-H4	6.8	6.7	6.6
<sup>3</sup> JCO4-H5	–	2.8	3.2
<sup>2</sup> JCO1-H1	5.0	5.2	5.4
<sup>3</sup> JCO1-H2	3.1	3.4	3.9
<sup>2</sup> JCO9-H9	–	4.0	4.7
<sup>3</sup> JCO3-H4	–	3.1	3.5
<sup>2</sup> JCO10-H10	5.8	5.2	5.7
<sup>3</sup> JCO10-H11	2.3	2.2	3.1
<sup>2</sup> JCO6-H6	3.8	3.8	4.2
<sup>3</sup> JCO6-H7	2.5	2.9	3.4
<sup>2</sup> JCO7-H7	4.9	4.4	ov.
<sup>2</sup> JCO11-H11	3.7	3.6	3.8
<sup>3</sup> JCO11-H1	1.9	2.7	3.3
<sup>2</sup> JCO2-H2	3.7	3.6	4.3
<sup>2</sup> JCO5-H5	2.6	2.9	3.6
<sup>3</sup> JCO5-H6	–	2.6	3.5
<sup>2</sup> JCO8-H8	3.1	3.1	3.5
<sup>3</sup> JCO8-H9	2.2	3.1	–

processed using the echo/anti-echo protocol. Sine bell shaped gradients of 1 ms duration were used, followed by a recovery delay of 20 μs. Prior to Fourier-transformation of each data, zero filling to 1024 in F1, 8192 points in F2 and a sine squared window function in both dimensions were applied. The analog 2D <sup>1</sup>H–<sup>13</sup>C HOBS-HSQMBC spectrum of Fig. 2B was recorded as described for

Fig. 2A using the detection period represented in Fig. 1A, with 20 loops (n), Δ = 28.25 ms and with the same selective pulse applied in the INEPT period.

All four spectra of Fig. 3 were recorded using the pulse sequence of Fig. 1B using only 64 t<sub>1</sub> increments, 4096 data points in t<sub>2</sub>, a 2.5 ms REBURP pulse as a region-selected <sup>13</sup>C pulse applied at

the CO region (172 ppm) to excite the carbonyl carbons and reducing the spectral width in the indirect F1 dimension to 1800 Hz. 2 scans were collected for each  $t_1$  increment and the overall experimental time for each 2D spectrum was about 5 min. In (A) a conventional detection period was used, in (B) and (D) broadband heteronuclear decoupling was achieved using a 4 kHz GARP scheme applied on-resonance to the carbonyl region, in (C) and (D)  $^1\text{H}$  homodecoupling (HOBS) was achieved using the detection period represented in Fig. 1A with 20 loops ( $n$ ) and  $\Delta = 28.25$  ms and with an acquisition time of 1.13 s. The spectrum of Fig. 5 was recorded as Fig. 3C but using 128  $t_1$  increments (experimental time of 10 min). The IPAP 2D subspectra of Fig. 6 were generated from the corresponding IP and AP-HSQMBC experiments separately acquired in the same conditions as described for Fig. 5, and data were added/subtracted in the time-domain without any scaling factor to provide spin-state selective data.

### Acknowledgments

Financial support for this research provided by MINECO (Project CTQ2012-32436) is gratefully acknowledged. We also thank to the Servei de Resonància Magnètica Nuclear, Universitat Autònoma de Barcelona, for allocating instrument time to this project.

### References

- [1] A. Bax, M.F. Summers, *J. Am. Chem. Soc.* 108 (1986) 2093–2094.
- [2] R.T. Williamson, B.L. Márquez, W.H. Gerwick, K.E. Kövér, *Magn. Reson. Chem.* 38 (2000) 265–273.
- [3] R.C. Crouch, T.D. Spitzer, G.E. Martin, *Magn. Reson. Chem.* 30 (1992) 595–605.
- [4] C. Gaillat, C. Lequart, P. Debeire, J.M. Nuzillard, *J. Magn. Reson.* 139 (1999) 454–459.
- [5] S. Yang, J.K. Gard, G. Harrigan, B. Parnas, J. Likos, R. Crouch, *Magn. Reson. Chem.* 41 (2003) 42–48.
- [6] K. Krishnamurthy, *J. Magn. Reson.* 153 (2001) 144–150.
- [7] R. Crouch, R.D. Boyer, R. Johnson, K. Krishnamurthy, *Magn. Reson. Chem.* 42 (2004) 301–307.
- [8] T.D.W. Claridge, I. Pérez-Victoria, *Org. Biomol. Chem.* 1 (2003) 3632–3634.
- [9] J. Furrer, *Chem. Comm.* 46 (2010) 3396–3398.
- [10] S. Gil, J.F. Espinosa, T. Parella, *J. Magn. Reson.* 207 (2010) 312–321.
- [11] J. Saurí, J.F. Espinosa, T. Parella, *Org. Biomol. Chem.* 11 (2013) 4473–4478.
- [12] A.J. Pell, J. Keeler, *J. Magn. Reson.* 189 (2007) 293–299.
- [13] B. Luy, *J. Magn. Reson.* 201 (2009) 18–24.
- [14] K. Zangger, H. Sterk, *J. Magn. Reson.* 124 (1997) 486–489.
- [15] N.H. Meyer, K. Zangger, *Angew. Chem. Intl. Ed.* 52 (2013) 7143–7146.
- [16] M. Nilsson, G.A. Morris, *Chem. Comm.* 9 (2007) 933–935.
- [17] J.A. Aguilar, S. Faulkner, M. Nilsson, G.A. Morris, *Angew. Chem. Intl. Ed.* 49 (2010) 3901–3903.
- [18] G.A. Morris, J.A. Aguilar, R. Evans, S. Haiber, M. Nilsson, *J. Am. Chem. Soc.* 132 (2010) 12770–12772.
- [19] J.A. Aguilar, A.A. Colbourne, J. Cassani, M. Nilsson, G.A. Morris, *Angew. Chem. Intl. Ed.* 51 (2012) 6460–6463.
- [20] A. Lupulescu, G.L. Olson, L. Frydman, *J. Magn. Reson.* 218 (2012) 141–146.
- [21] J.A. Aguilar, M. Nilsson, G.A. Morris, *Angew. Chem. Intl. Ed.* 50 (2011) 9716–9717.
- [22] P. Sakhaei, B. Haase, W. Bermel, *J. Magn. Reson.* 228 (2013) 125–129.
- [23] L. Castañar, P. Nolis, A. Virgili, T. Parella, *Chem. Eur. J.* (2013) in press. <http://dx.doi.org/10.1002/chem.201303235>.
- [24] T. Parella, J.F. Espinosa, *Prog. Nucl. Magn. Reson. Spectrosc.* 73 (2013) 17–55.
- [25] B. Yu, H. van Ingen, S. Vivekanandan, C. Rademacher, S.E. Norris, D.I. Freedberg, *J. Magn. Reson.* 215 (2012) 10–22.
- [26] B. Yu, H. van Ingen, D.I. Freedberg, *J. Magn. Reson.* 228 (2013) 159–165.
- [27] J. Farjon, W. Bermel, C. Griesinger, *J. Magn. Reson.* 180 (2006) 72–82.
- [28] V.M. Marathias, I. Goljer, A.C. Bach II, *Magn. Reson. Chem.* 43 (2005) 512–519.
- [29] C.M. Thiele, W. Bermel, *J. Magn. Reson.* 216 (2012) 134–143.
- [30] L. Paudel, R.W. Adams, P. Kiraly, J.A. Aguilar, M. Foroozandeh, M.J. Cliff, M. Nilsson, P. Sandor, J.P. Waltho, G.A. Morris, *Angew. Chem. Intl. Ed.* 52 (2013) 11616–11619.
- [31] L. Kaltschnee, A. Kolmer, I. Timári, R.W. Adams, M. Nilsson, K.E. Kövér, G.A. Morris, C.M. Thiele, Pure Shift HSQC Measurements with Perfect BIRD Decoupling – A Method to Decouple Diastereotopic Protons, Poster No. 391 Presented at 9th European Magnetic Resonance Conference EUROMAR, 2013.
- [32] I. Timári, L. Kaltschnee, A. Kolmer, R.W. Adams, M. Nilsson, C.M. Thiele, G.A. Morris, K.E. Kövér, *J. Magn. Reson.*, in press. <http://dx.doi.org/10.1016/j.jmr.2013.10.023>.
- [33] J. Saurí, J.F. Espinosa, T. Parella, *Angew. Chem. Intl. Ed.* 51 (2012) 3919–3922.